

HETEROCYCLES, Vol. 102, No. 2, 2021, pp. 254 - 273. © 2021 The Japan Institute of Heterocyclic Chemistry
Received, 9th December, 2020, Accepted, 23rd December, 2020, Published online, 6th January, 2021
DOI: 10.3987/COM-20-14391

[2+2]PHOTOCYCLOADDITION OF 5,6-SUBSTITUTED 2-OXO-2H-PYRAN-3-CARBOXYLATES WITH ALKENES

Yun-Han Hsieh, Hiroki Iwasaki, Yumina Iwai, Miki Adachi, Kanako Kitai, Eri Kuribayashi, Yuri Hirata, Suzuna Sakaguchi, Naoko Sakaguchi, Naoto Kojima, and Masayuki Yamashita*

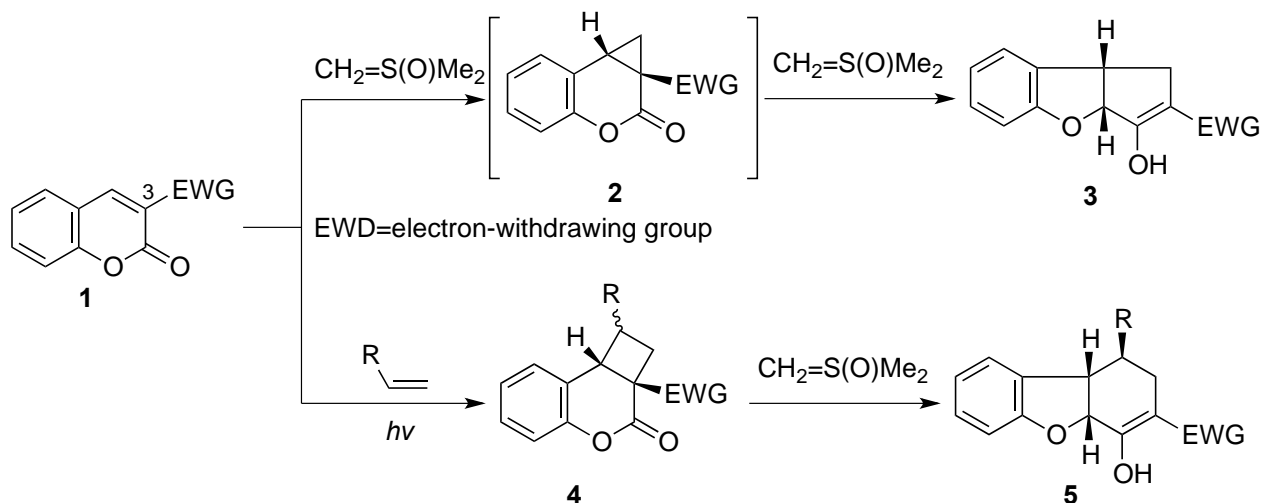
Kyoto Pharmaceutical University, 1 Misasagi-Shichono-cho, Yamashina, Kyoto 607-8412, Japan; E-mail: yamasita@mb.kyoto-phu.ac.jp

Abstract – The [2+2]photocycloaddition of alkenes and 5,6-substituted 2-oxo-2H-pyran-3-carboxylates with an ester as an electron-withdrawing group was developed. The 3,4-adducts, 4,5-disubstituted 3-oxa-2-oxobicyclo[4.2.0]oct-4-ene-1-carboxylates, were obtained in moderate yields accompanied by considerable amounts of the 5,6-adducts, 1,6-disubstituted 2-oxa-3-oxobicyclo[4.2.0]oct-4-ene-4-carboxylates. These structures, including their stereochemistry, were determined by various spectral and computational analyses, and some were examined by X-ray crystallographic analysis. The determined regio- and stereoselectivities were explained by frontier orbital theory.

INTRODUCTION

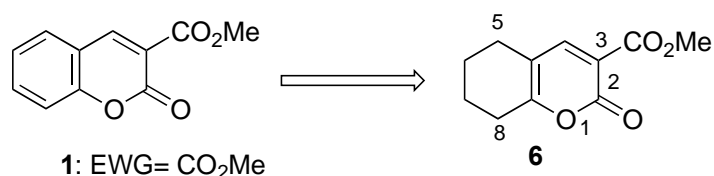
Small-ring cycloalkanes, such as cyclopropanes and cyclobutanes, are basic structural constituents in a wide range of natural products.^{1,2} In organic synthesis, these cycloalkanes also play important roles owing to the diversity of their reactions, and they have high reactivities toward ring-opening reactions that are attributable to both angle and torsional strains.^{3,4} Thus, cyclopropanes and cyclobutanes undergo reactions such as ring-opening to acyclic compounds and ring enlargement. Furthermore, it is also possible for ring contraction to cyclopropanes to occur in cyclobutanes. For these reasons, many organic chemists have taken note of small cycloalkanes.

We have been interested in the reactivity of small-ring compounds and have reported reactions proceeding via cyclopropane intermediates prepared from coumarin derivatives bearing an electron-withdrawing group at the 3-position (**1**) with dimethylsulfoxonium methylide ($\text{CH}_2=\text{S}(\text{O})\text{Me}_2$)^{5,6} and cyclobutane derivatives (**4**) prepared from **1** with $\text{CH}_2=\text{S}(\text{O})\text{Me}_2$ (Scheme 1).⁷

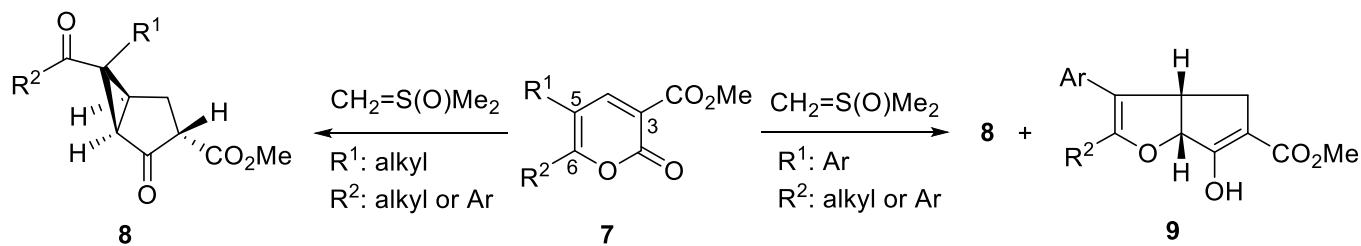


Scheme 1. Our previous report

5,6,7,8-Tetrahydro-2-oxo-2*H*-1-benzopyran-3-carboxylate (**6**) can be regarded as a compound that has lost the aromaticity of the benzene ring of **1** (electron-withdrawing group = CO₂Me) (Scheme 2). Next, we focused on other 2-oxo-2*H*-pyran-3-carboxylates like **6**. The 2*H*-1-pyran-2-one ring system is present in a number of natural products⁸ and biologically active compounds, such as the nonpeptide protease inhibitor of human immunodeficiency virus-1⁹; it is also involved in root architecture regulation¹⁰ and plant growth promotion¹¹ and exhibits antifungal activity¹² and antibacterial activity.¹³ It is also a useful building block in organic synthesis as a scaffold for $\alpha,\beta,\gamma,\delta$ -conjugated lactone groups within a six-membered ring.¹⁴

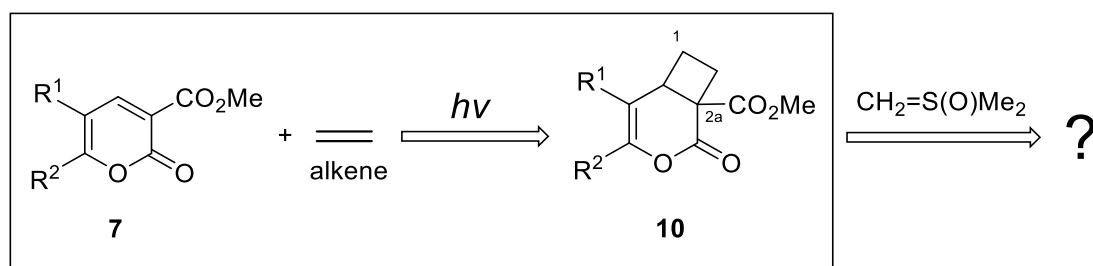
Scheme 2. Structural similarity of 5,6,7,8-tetrahydro-2-oxo-2*H*-1-benzopyran-3-carboxylate and 2-oxo-2*H*-1-benzopyran-3-carboxylate

Recently, we developed a reaction of 2-oxo-2*H*-pyran-3-carboxylates with an ester as the electron-withdrawing group at the 3-position (**7**) with CH₂=S(O)Me₂, which proceeded via the cyclopropane intermediates. Interestingly, different products were obtained depending on the substituent group at the 5-position. With alkyl groups as the substituent, only **8** was produced. On the other hand, with aryl groups, both **9** and **8** were obtained (Scheme 3).¹⁵



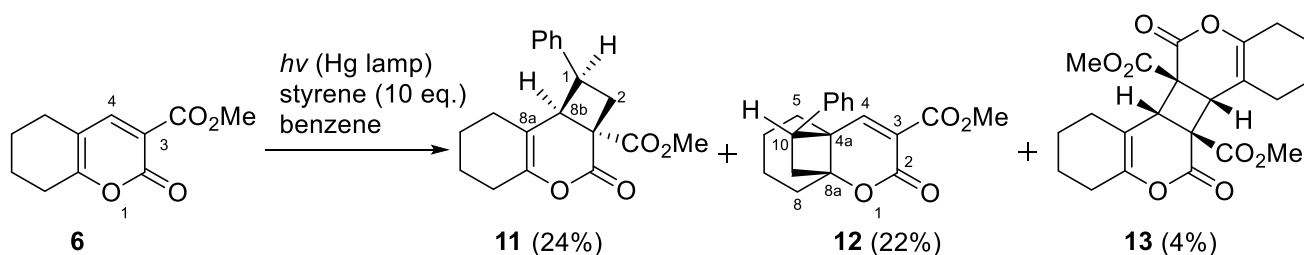
Scheme 3. Our previous report

Next, we were interested in the reaction of the cyclobutane derivatives (**10**) with $\text{CH}_2=\text{S}(\text{O})\text{Me}_2$ (Scheme 4). However, to the best of our knowledge, cyclobutane compounds such as **10**, which have an electron-withdrawing group at the 2a-position, have not been reported. Some methods for the synthesis of cyclobutane derivatives from 2*H*-pyran-2-ones with themselves and/or alkenes by [2+2]photocycloaddition have been reported.^{16,17} The [2+2]photocycloaddition of alkenes is a highly useful methodology for the preparation of cyclobutane compounds in organic synthesis because of the formation of two new carbon–carbon bonds that introduce four new stereocenters at a maximum.¹⁸ In this paper, the preparation of **10** from **7** by [2+2]photocycloaddition is reported.

Scheme 4. Synthetic plan for **10** by [2+2]photocycloaddition

RESULTS AND DISCUSSION

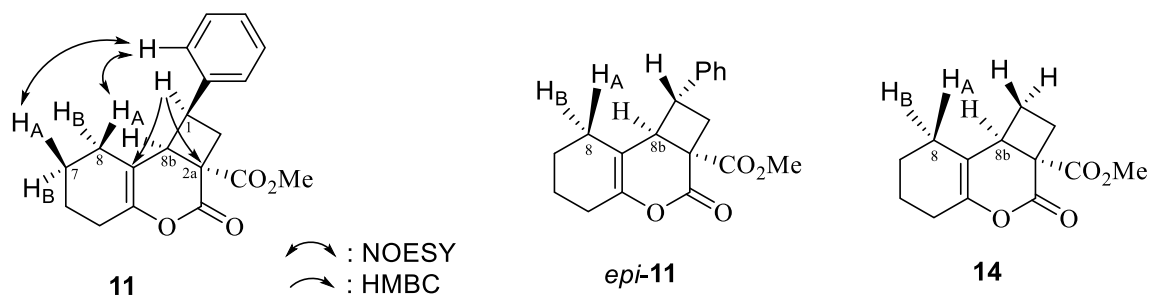
We previously reported the [2+2]photocycloaddition of coumarin-3-carboxylates (**1**) and alkenes.^{7,19} According to this procedure, a solution of **6** and 10 equivalents of styrene in benzene was irradiated with a high-pressure mercury lamp (400 W) to afford the [2+2]cycloadducts. The 3,4-adduct (**11**), 5,6-adduct (**12**), and dimer of **6** (**13**) were isolated in 24%, 22%, and 4% yields, respectively (Scheme 5).¹⁰

Scheme 5. [2+2]Photocycloaddition of **6** and styrene

The structures of **11–13** were determined by spectroscopy, X-ray crystallography, and/or computational chemistry. The molecular formulae of **11** and **12** were both $C_{19}H_{20}O_4$ based on high-resolution electron impact mass spectrometry, which corresponds to the adduct of **6** and styrene. On the other hand, the formula of **13** was $C_{22}H_{24}O_8$, which corresponds to a dimer of **6**. The positions of the cyclobutane rings in **11** and **12** were established by comparison with their $^1\text{H-NMR}$ spectra. In the $^1\text{H-NMR}$ spectra of **11** and **12**, the protons on the cyclobutane ring were specifically observed between 2.0 and 4.0 ppm regardless of other protons. For **12**, the number of hydrogen atoms on the cyclobutane ring was three, and the signal corresponding to 4-H, the β -hydrogen atom of the α,β -unsaturated dicarbonyl compound, was observed at 6.85 ppm as a singlet. The same signal in the spectrum of **6** was observed at 8.04 ppm. On the other hand, for **11**, the number of hydrogen atoms on the cyclobutane ring was four, and the downfield-shifted signal at approximately 6–7 ppm, similar to 4-H in **6**, was not observed. Consequently, it was determined that **11** was the 3,4-adduct and **12** was the 5,6-adduct. The position of the phenyl group in **11** was determined by the coupling pattern of hydrogen atoms on the cyclobutane ring in the $^1\text{H-NMR}$ spectrum, the signals of which were observed as doublet of doublet of doublets (ddd) for 1-H, a doublet of doublets (dd) for the two 2-Hs, and a doublet (d) for 8b-H. Furthermore, interactions between 1-H and 8a-C and between 1-H and 2a-C in the heteronuclear multiple bond coherence (HMBC) spectrum were observed. As **11** was a sole product, the stereochemistry of the phenyl group could not be determined based on the spectral comparison between **11** and its 1-epimer (*epi-11*). The stereochemistry of the phenyl group of **11** was presumed by $^1\text{H-NMR}$ spectral prediction of density functional theory (DFT) calculations of **11**, *epi-11*, and the cyclobutane compound without the phenyl group (**14**).²⁰ In the calculated $^1\text{H-NMR}$ spectra, the chemical shifts for 8- H_A and 8- H_B were predicted as 1.02 and 1.38 for **11**, 1.40 and 1.85 for *epi-11*, and 1.98 and 1.76 for **14**, respectively. For *epi-11* and **14**, where there was no phenyl ring influence, the signals of 8- H_A and 8- H_B were predicted to appear at approximately 1.4–2.0 ppm; on the other hand, those in the calculated **11** spectrum shifted to the higher field at 1.02 and 1.38 ppm due to the shielding effect of the phenyl ring. In reality, the signals of 8- H_A and 8- H_B in **11** were observed at 0.92–0.98 and 1.46–1.51 ppm, respectively (Table 1). The stereochemistry of the phenyl group of **11** was established by observing the interactions between 7- H_A and Ph-H and between 8- H_A and Ph-H via nuclear Overhauser

effect spectroscopy (NOESY). From these results, **11** was determined to be methyl *rac*-(1*R*,2*aS*,8*bS*)-3-oxo-1-phenyl-1,5,6,7,8,8*b*-hexahydro-2*H*-cyclobuta[*d*]cyclohexa[*b*]pyran-2*a*(3*H*)-carboxylate.

Table 1. Comparison of the ^1H -NMR chemical shifts of **11** and calculated shifts for **11**, *epi*-**11**, and **14**

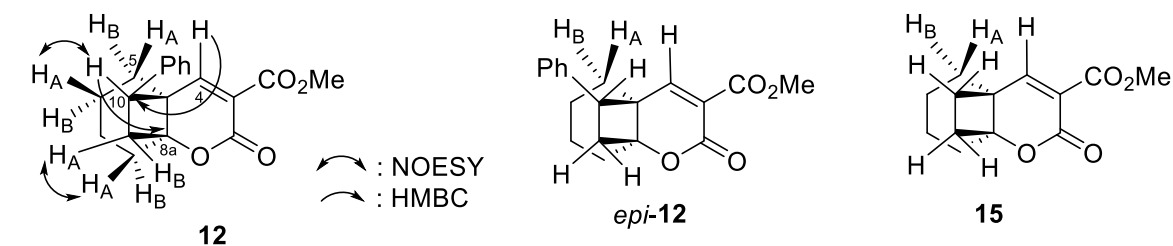


Position	Chemical shift (ppm)			
	Observed 11	Calculated 11 ^a	Calculated <i>epi</i> - 11 ^a	Calculated 14 ^a
8- H_A	0.92–0.98 (0.95 ^b)	1.02	1.40	1.98
8- H_B	1.46–1.51 (1.49 ^b)	1.38	1.85	1.76
8 <i>b</i> -H	3.42	3.43	2.98	2.76

a: DFT calculations were performed at the $\omega\text{B97X-D/6-31G}^*$ level of theory.

b: Median value.

Although the position of the phenyl group in **12** could not be determined using the coupling pattern of hydrogens on the cyclobutane ring in the ^1H -NMR spectrum, it was established by observing the interactions between 4-H and 10-C and between 10-H and 8*a*-C in the HMBC spectrum. As **12** was a sole product, the stereochemistry of the phenyl group could not be determined based on the spectral comparison between **12** and its 10-epimer (*epi*-**12**). The stereochemistry of the phenyl group was assumed by ^1H -NMR spectral prediction of the DFT calculations of **12**, *epi*-**12**, and the cyclobutane compound without a phenyl group (**15**). The protons at the 4- and 5-positions in **12** and *epi*-**12** should be strongly influenced by the phenyl group. The observed chemical shifts of 4-H, 5- H_A , and 5- H_B were compared with the calculated values for **12**, *epi*-**12**, and **15** and found to be close to the calculated values of **12** (Table 2). The stereochemistry of the phenyl group of **12** was established by observing the interactions between 6- H_A and 10-H and between 8- H_A and 9- H_A via NOESY. From these results, **12** was determined to be methyl *rac*-(4*aR*,8*aS*,10*S*)-5,6,7,8-tetrahydro-2-oxo-10-phenyl-4*a*,8*a*-ethano-2*H*-1-benzopyran-3-carboxylate.

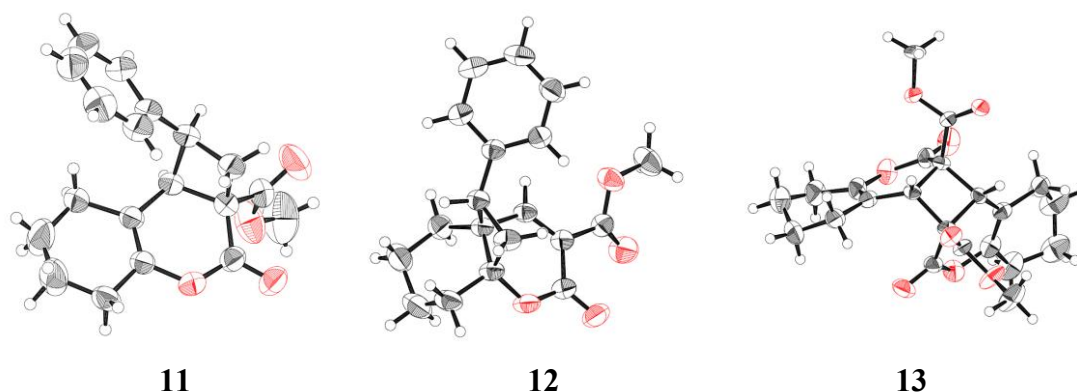
Table 2. Comparison of the $^1\text{H-NMR}$ chemical shifts of **12** and calculated shifts for **12**, *epi-12*, and **15**

Position	Chemical shift (ppm)			
	Observed 12	Calculated 12 ^a	Calculated <i>epi-12</i> ^a	Calculated 15 ^a
4-H	6.85	6.69	7.64	7.48
5-H _A	1.81–1.93 (1.87 ^b)	1.63	1.39	1.53
5-H _B	1.24–1.43 (1.34 ^b)	1.19	1.38	1.27

a: DFT calculations were performed at the $\omega\text{B97X-D/6-31G}^*$ level of theory.

b: Median value.

Finally, the structures of **11**, **12**, and **13**, including their stereochemistry, were confirmed by X-ray crystallography (Figure 1). Compound **13** was found to be the dimer of **6**, as well as the *syn*-head to tail adduct.

Figure 1. ORTEP drawings of **11**, **12**, and **13**

The regio- and stereoselectivities of **11** and **12** were explained by frontier orbital theory. Generally, in a photoreaction, the frontier orbitals, i.e., the HOMO and LUMO, of each of the two reactants in the ground state interact. Namely, the important frontier orbitals are the HOMO/'HOMO' and LUMO/'LUMO', where single quotation marks indicate the orbitals in the ground state before photoexcitation, not the actual orbitals during the reaction.²¹ The molecular orbitals of **6** and styrene were calculated at the

ω B97X-D/6-31G* level of DFT. The energy gap between the HOMOs of **6** (−8.3 eV) and styrene (−8.0 eV) was lower than that of the LUMOs (−0.1 and 1.1 eV, respectively). Therefore, this cycloaddition reaction should proceed via the interaction between the HOMO of **6** and ‘HOMO’ of styrene. The 3,4-adduct was preferred over the 5,6-adduct. Regarding the regioselectivity, the orbital overlap of the 3,4-addition of **6** and styrene is more suitable than the 5,6-addition. Their stereoselectivities were described by the secondary orbital interaction between the γ,δ -double bond of **6** and the benzene ring of styrene for the 3,4-addition and between the α,β -double bond of **6** and the benzene ring of styrene for the 5,6-addition. Although the production of **13** is disadvantageous with respect to orbital overlap, the reaction proceeds to avoid steric hindrance (Figure 2).

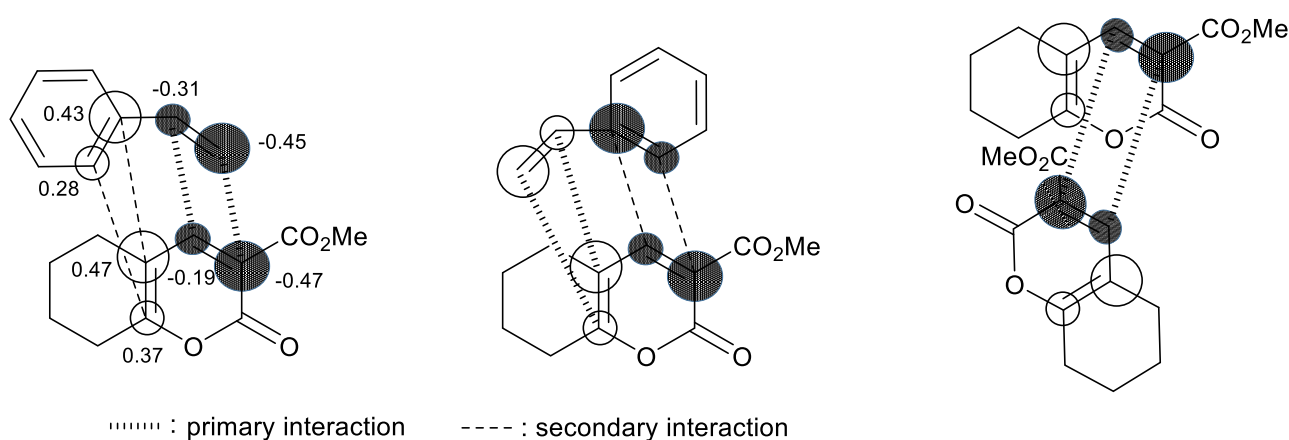


Figure 2. Interaction of frontier orbitals. The coefficients were calculated at the STO-3G level of theory using the Hartree–Fock method.

The photoreaction with different solvents and amounts of styrene were then investigated, and the results are shown in Table 3. Solvents were first tested, and the 3,4-adduct **11** was the major product in all solvents and neat (entries 1–11). The highest yield of **11** was neat, while the yield in isopropanol was comparable to that in neat. Isopropanol was chosen as the solvent for further reaction because of its ease of handling. Next, the amount of styrene was studied. As the amount of styrene increased, the yield of **11** gradually increased (entries 11–16). However, there was almost no change above 10 equivalents.

The reaction conditions for entry 11 in Table 3 were applied to various 2-oxo-2*H*-pyran-3-carboxylates (**16**) and alkenes, and the results are shown in Table 4. Except for entries 10, 13, and 14, the 3,4-adducts (**17**) were the major product, along with considerable amounts of the 5,6-adducts (**18**). In entries 6 and 18, the 5,6-adducts were not obtained. The structures and stereochemistry of **17** and **18** were confirmed by comparison with the $^1\text{H-NMR}$ spectra of **11** and **12**. In particular, the proton signals around the cyclobutane ring of **11** and **12** were characteristic. In the $^1\text{H-NMR}$ spectra of **17** and **18**, similar signal patterns were observed around the cyclobutane ring. Some of the compounds were analyzed by X-ray crystallography.

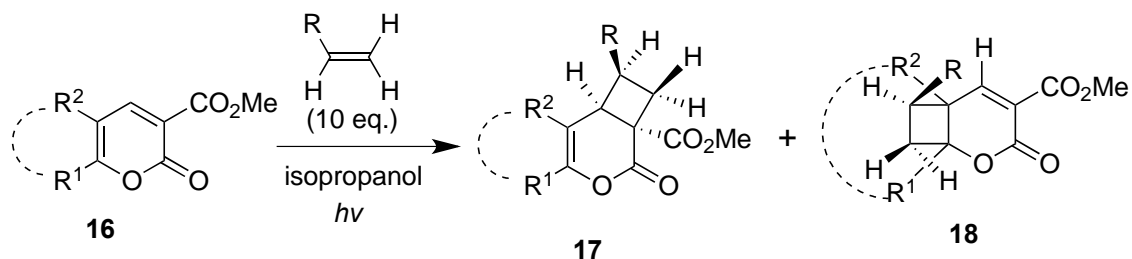
Table 3. Examination of solvents and amounts of styrene

Entry	Solvent	Styrene (eq.)	Time ^a (h)	Yield (%)		
				11	12	13
1	Benzene	10	10	24	22	4
2	Toluene	10	23	49	27	8
3	Acetonitrile	10	11	51	40	2
4	Dichloromethane	10	29	52	35	Trace
5	Cyclohexane	10	11	44	19	13
6	Tetrahydrofuran	10	12	47	34	4
7	Acetone	10	9	51	30	Trace
8	Ethyl acetate	10	14	42	27	4
9	Dimethylformamide	10	10	43	29	3
10	Neat	10	15	56	29	Trace
11	Isopropanol	10	9	55	30	4
12	Isopropanol	1	9	38	25	6
13	Isopropanol	2	9	43	30	3
14	Isopropanol ^b	3	9	48	42	Trace
15	Isopropanol	5	9	51	39	3
16	Isopropanol	15	9	50	32	Trace

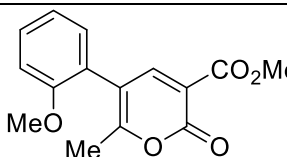
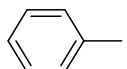
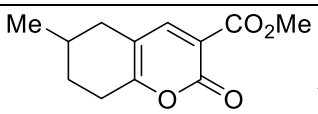
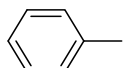
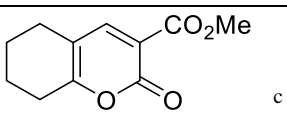
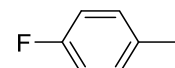
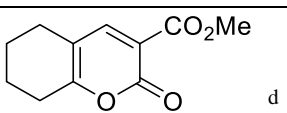
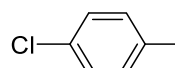
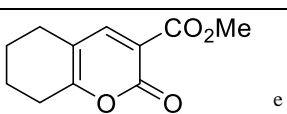
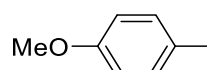
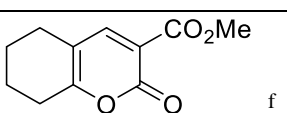
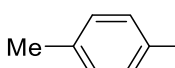
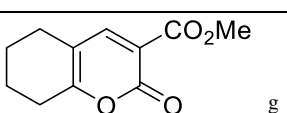
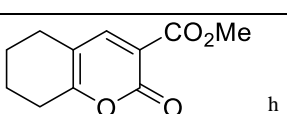
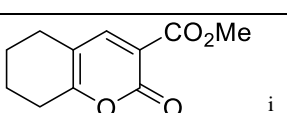
a: The time when **6** disappeared by TLC check.

b: Compound **6** was added in quarters.

The substituent groups at the 5,6-positions were acceptable regardless of the presence of acyclic or cyclic groups (entries 1–15, 18) and aliphatic or aromatic groups (entries 8–10). The various substituent groups on the benzene ring of the substituted styrenes were also acceptable (entries 12–15). When *n*-1-hexene and 1-*n*-octene were used as alkenes, only the dimer of **13** was afforded (entries 16 and 17). On the other hand, when 1,3-butadiene was used as the alkene, the 3,4-adduct was obtained in 21% yield without the 5,6-adduct (entry 18). These results showed that the secondary interaction of the frontier orbitals is important in this reaction.

Table 4. [2+2]Photocycloaddition of 2-oxo-2*H*-pyran-3-carboxylates (**16**) with alkenes

Entry	Substrate	 R-	Time (h)	Yield (%)	
				17	18
1	16a:		9	17a: 42 ^j	18a: 22
2	16b:		13	17b: 45	18b: 30 ^j
3	16c:		9	17c: 53 ^j	18c: 28 ^j
4	16d:		13	17d: 58 ^j	18d: 35 ^j
5^a	16e:		10	17e: 32	18e: 25
6^a	16f:		15	17f: 50 ^j	-
7	16g:		15	17g: 47	18g: 28 ^j
8	16h:		21	17h: 21	18h: 18
9	16i:		21	17i: 17	18i: 5

10	16j: 		44	17j: 20	18j: 22
11	16k:  b		9	17k: 63 ^k	18k: 30 ^{j,k}
12	6:  c		9	17l: 39	18l: 37
13	6:  d		5	17m: 31	18m: 45
14	6:  e		11	17n: 27	18n: 48
15	6:  f		9	17o: 38	18o: 36
16	6:  g	Me(CH ₂) ₃ -	10	-	-
17	6:  h	Me(CH ₂) ₅ -	11	-	-
18 ^l	6:  i	H ₂ C=CH-	10	17p: 21 ^l	-

a: Ethyl acetate was used as a solvent.

b: The dimer of **16l** was obtained in 5% yield as a diastereomeric mixture.

c–i: The dimer (**13**) was obtained (c: 4%, d: 4%, e: 3%, f: 4%, g: 14%, h: 17%, i: 21%)

j: The structure was confirmed by X-ray crystallography.

k: Diastereomeric mixtures of 6 : 4.

l: The reaction was carried out in a sealed tube.

In conclusion, the [2+2]photocycloaddition reaction of 2-oxo-2*H*-pyran-3-carboxylates with an ester group at the 3-position and conjugated alkenes was developed. The 3,4-adducts were obtained in moderate yields accompanied by considerable amounts of the 5,6-adducts. These structures, including their stereochemistry, were determined by various spectral and computational analyses, and some were

investigated by X-ray crystallographic analyses. The regio- and stereochemistry were explained by the HOMO/'HOMO' interaction in frontier orbital theory. Studies are now ongoing in our group for the use of the 3,4-adducts as starting compounds, and the results will be presented in due course.²²

EXPERIMENTAL

GENERAL: Melting points were measured with a Yanaco MP micro-melting point apparatus and are uncorrected. NMR spectra were measured on Bruker Ultrashield™ 300 (¹H: 300 MHz; ¹³C: 75 Hz), JEOL ECS-400 (¹H: 400 MHz; ¹³C: 100 Hz), and Bruker Ascend™ 500 (¹H: 500 MHz; ¹³C: 125 Hz) spectrometers with tetramethylsilane as the internal standard. Chemical shifts are reported in parts per million. IR spectra were measured with a JASCO FT/IR-4600 spectrophotometer. A JEOL JMS-GC mate II spectrometer was used for low-resolution and high-resolution electron ionization mass spectrometry (LR-EIMS and HR-EIMS). X-Ray crystal analyses were performed on a Rigaku RAXIS RAPID II imaging plate area detector with graphite monochromatized Cu-K α or Mo-K α radiation at 23.0 °C. Photochemical reactions were performed on an RH-400-10W (Riko-Kagaku Sangyo). All solvents were removed under reduced pressure in the usual work-up procedure. Silica gel 60 F₂₅₄ (Merck) for thin-layer chromatography, silica gel 60N (Kanto Chemical) for column chromatography, silica gel packed in a glass column (Yamazen, 0.040 mm) for medium-pressure liquid chromatography (MPLC), Cosmosil 5SL-II, and Cosmosil 5C₁₈-AR-II packed column (Nacalai Tesque, 20 mm I.D. \times 250 mm) for recycling preparative high-performance liquid chromatography (HPLC) were used.

TYPICAL PROCEDURE FOR THE SYNTHESIS OF METHYL *rac*-(1*R*,2*aS*,8*bS*)-3-OXO-1-PHENYL-1,5,6,7,8,8*b*-HEXAHYDRO-2*H*-CYCLOBUTA[*d*]CYCLOHEX[*b*]PYRAN-2*a*(3*H*)-CARBOXYLATE (11), METHYL *rac*-(4*aR*,8*aS*,10*S*)-5,6,7,8-TETRAHYDRO-2-OXO-10-PHENYL-4*a*,8*a*-ETHANO-2*H*-1-BENZOPYRAN-3-CARBOXYLATE (12), AND DIMETHYL *rac*-(6*aR*,6*bS*,12*aR*,12*bS*)-6,12-DIOXO-2,3,4,7,8,9,10,12*b*-OCTAHYDRO-1*H*,6*H*-CYCLOBUTA[1,2-*c*:3,4-*c'*]BIS[1]BENZOPYRAN-6*a*,12*a*(6*aH*,12*bH*)-DICARBOXYLATE (13): A mixture of methyl 5,6,7,8-tetrahydro-2-oxo-2*H*-1-benzopyran-3-carboxylate (**6**, 1.0 mmol) and styrene (10.0 eq.) in 2-propanol (5.0 mL) was irradiated with a high-pressure mercury lamp (400 W) to afford the [2+2] cycloadducts until **6** disappeared as determined by TLC (9–29 h). The reaction mixture was evaporated under reduced pressure. The residue was chromatographed on silica gel with *n*-hexane-EtOAc as the eluent to give the corresponding compounds **11**, **12**, and **13**.

11: Colorless plates; mp 114.4–115.2 °C (diisopropyl ether); ¹H-NMR (500 MHz, CDCl₃) δ 7.31 (t, *J* = 7.5 Hz, 2H), 7.27–7.24 (m, 1H), 7.20 (d, *J* = 7.5 Hz, 2H), 3.91 (q, *J* = 9.0 Hz, 1H), 3.85 (s, 3H), 3.42 (d, *J*

= 9.0 Hz, 1H), 3.34 (ddd $J = 11.5, 9.5, 2.0$ Hz, 1H), 2.89 (dd, $J = 13.0, 8.0$ Hz, 1H), 2.10 (td, $J = 6.0, 2.0$ Hz, 2H), 1.58-1.52 (m, 1H), 1.51-1.39 (m, 2H), 1.34-1.27 (m, 1H), 1.07-0.99 (m, 1H), 0.98-0.92 (m, 1H); ^{13}C -NMR (75 MHz, CDCl_3) δ 170.9, 166.2, 146.7, 138.6, 128.2 (2C), 127.9 (2C), 127.2, 106.8, 53.2, 47.7, 46.5, 41.2, 33.9, 26.2, 25.8, 21.9, 21.7; IR (ATR): 3029.6, 1739.5 cm^{-1} ; LR-EIMS m/z : 312 (M^+ , 1.0), 208 (100), 180 (40), 176 (14), 152 (13), 121 (22), 104 (14).; HR-EIMS calcd for $\text{C}_{19}\text{H}_{20}\text{O}_4$: 312.1362. Found: 312.1363.

X-Ray Crystal Data: Crystal Color, Habit; colorless, block, Crystal Dimensions; 0.400 x 0.300 x 0.300 mm, Crystal System; monoclinic, Lattice Type; Primitive, Lattice Parameters; $a = 11.1831(2)$ Å, $b = 9.6074(2)$ Å, $c = 15.8510(3)$ Å, $\beta = 103.284(7)^\circ$, $V = 1657.47(8)$ Å³, Space Group; $\text{P}2_1/\text{n}$ (#14), Z value; 4, D_{calc} ; 1.252 g/cm^3 , F_{000} ; 664.00, $\mu(\text{CuK}\alpha)$; 7.105 cm^{-1} , Intensity Measurement: Diffractometer; R-Axis RAPID, Radiation; $\text{CuK}\alpha$ ($\lambda = 1.54187$ Å), graphite monochromated, Voltage, Current; 40 kV, 100 mA, Temperature; 23.0 °C, Detector Aperture; 460.0 x 256.0 mm, Data Images; 45 exposures, ω oscillation Range ($\chi=54.0$, $\phi=0.0$); 80.0 - 260.0°, Exposure Rate; 140.0 $\text{sec}/^\circ$, ω oscillation Range ($\chi=54.0$, $\phi=90.0$); 80.0 - 260.0°, Exposure Rate; 140.0 $\text{sec}/^\circ$, ω oscillation Range ($\chi=54.0$, $\phi=180.0$); 80.0 - 260.0°, Exposure Rate; 140.0 $\text{sec}/^\circ$, ω oscillation Range ($\chi=54.0$, $\phi=270.0$); 80.0 - 260.0°, Exposure Rate; 140.0 $\text{sec}/^\circ$, Detector Position; 127.40 mm, Pixel Size; 0.100 mm, $2\theta_{\text{max}}$; 136.1°, No. of Reflections Measured; Total: 17813, Unique: 2988 ($R_{\text{int}} = 0.0531$), Corrections; Lorentz-polarization Absorption (trans. factors: 0.692 - 0.808), Secondary Extinction (coefficient: 9.39000e-003). Structure Solution; Direct Methods (SHELXT Version 2018/2), Refinement; Full-matrix least-squares on F^2 , Function Minimized; $\Sigma w(\text{Fo}^2 - \text{Fc}^2)^2$, Least Squares Weights; $w = 1/[\sigma^2(\text{Fo}^2) + (0.0618 \cdot P)^2 + 0.2621 \cdot P]$ where $P = (\text{Max}(\text{Fo}^2, 0) + 2\text{Fc}^2)/3$, $2\theta_{\text{max}}$ cutoff; 136.1°, Anomalous Dispersion; All non-hydrogen atoms, No. Observations (All reflections); 2988, No. Variables; 228, Reflection/Parameter Ratio; 13.11, Residuals: R_1 ($I > 2.00\sigma(I)$); 0.0415, Residuals: R (All reflections); 0.0451, Residuals: wR_2 (All reflections); 0.1194, Goodness of Fit Indicator; 1.046, Max Shift/Error in Final Cycle; 0.000, Maximum peak in Final Diff. Map; 0.18 $\text{e}^-/\text{Å}^3$, Minimum peak in Final Diff. Map; -0.15 $\text{e}^-/\text{Å}^3$.

Deposition number CCDC-2047464 for **11**. Free copies of the data can be obtained via <http://www.ccdc.cam.ac.uk/conts/retrieving.html> (or from the Cambridge Crystallographic Data Center, 12 Union Road, Cambridge, CB2 1EZ, UK; Fax: +44 1223 336033; e-mail: deposit@ccdc.cam.ac.uk).

Selected Bond Lengths (Å)

O1-C9	1.4135(17)	O1-C1	1.3460(15)	O2-C1	1.1992(19)
O3-C18	1.326(2)	O3-C19	1.442(2)	C4-C5	1.5103(19)

C4-C9	1.3223(17)	C4-C3	1.4929(16)	C5-C6	1.515(4)
C5-C6A	1.531(4)	C6-C7	1.522(7)	C7-C8	1.555(6)
C9-C8	1.4932(18)	C10-C11	1.545(2)	C10-C2	1.552(2)
C11-C12	1.496(2)	C11-C3	1.5780(19)	C12-C13	1.392(2)
C12-C17	1.387(2)	C13-C14	1.382(3)	C14-C15	1.370(3)
C15-C16	1.374(3)	C16-C17	1.389(3)	C18-O4	1.192(2)
C18-C2	1.517(2)	C1-C2	1.5032(19)	C2-C3	1.5633(19)
C8-C7A	1.464(8)	C7A-C6A	1.496(10)		

Selected Bond Angles (°)

C9-O1-C1	122.16(10)	C18-O3-C19	117.66(16)	C5-C4-C9	120.01(10)
C5-C4-C3	117.65(10)	C9-C4-C3	122.27(12)	C4-C5-C6	113.98(19)
C4-C5-C6A	109.8(3)	C5-C6-C7	109.9(4)	C6-C7-C8	109.7(4)
O1-C9-C4	124.23(11)	O1-C9-C8	109.15(11)	C4-C9-C8	126.60(13)
C11-C10-C2	89.17(11)	C10-C11-C12	121.39(12)	C10-C11-C3	88.34(10)
C12-C11-C3	120.35(11)	C11-C12-C13	119.12(13)	C11-C12-C17	122.69(13)
C13-C12-C17	118.13(16)	C12-C13-C14	120.83(15)	C13-C14-C15	120.41(18)
C14-C15-C16	119.7(2)	C15-C16-C17	120.38(17)	C12-C17-C16	120.57(15)
O3-C18-O4	124.68(15)	O3-C18-C2	110.13(12)	O4-C18-C2	125.19(16)
O1-C1-O2	118.30(12)	O1-C1-C2	118.12(12)	O2-C1-C2	123.49(12)
C10-C2-C18	113.90(11)	C10-C2-C1	113.51(11)	C10-C2-C3	88.64(11)
C18-C2-C1	108.96(12)	C18-C2-C3	112.30(11)	C1-C2-C3	118.49(10)
C4-C3-C11	116.31(11)	C4-C3-C2	112.23(10)	C11-C3-C2	87.60(9)
C7-C8-C9	110.3(2)	C9-C8-C7A	111.7(3)	C8-C7A-C6A	111.7(5)
C5-C6A-C7A	111.6(5)				

12: Colorless needles; mp 126.9-128.4 °C (diisopropyl ether); ¹H-NMR (300 MHz, CDCl₃) δ 7.38-7.25 (m, 3H), 7.12-7.08 (m, 2H), 6.85 (s, 1H), 3.77 (s, 3H), 3.52 (dd, *J* = 10.8, 7.2 Hz, 1H), 2.80 (t, *J* = 10.8 Hz, 1H), 2.37 (ddd, *J* = 14.7, 4.2, 3.3 Hz, 1H), 2.28 (dd, *J* = 11.1, 7.5 Hz, 1H), 1.95-1.81 (m, 3H), 1.77-1.57 (m, 2H), 1.43-1.24 (2H, m); ¹³C-NMR (125 MHz, CDCl₃) δ 163.8, 159.4, 156.3, 135.2, 128.7 (2C), 127.5 (2C), 127.4, 122.9, 77.0, 52.5, 48.4, 38.8, 36.9, 34.6, 28.8, 20.6, 20.4; IR (ATR): 3025.8, 1753.0, 1713.4 cm⁻¹; LR-EIMS *m/z*: 312 (M⁺, 1.0), 208 (100), 180 (44), 176 (16), 152 (15), 121 (24), 104 (15).; HR-EIMS calcd for C₁₉H₂₀O₄: 312.1362. Found: 312.1357.

X-Ray Crystal Data: Crystal Color, Habit; colorless, platelet, Crystal Dimensions; 0.200 x 0.100 x 0.040 mm, Crystal System; triclinic, Lattice Type; Primitive, Lattice Parameters; $a = 9.2261(5) \text{ \AA}$, $b = 10.5187(6) \text{ \AA}$, $c = 10.5900(5) \text{ \AA}$, $\alpha = 104.403(7)^\circ$, $\beta = 103.284(7)^\circ$, $\gamma = 107.817(8)^\circ$, $V = 802.79(14) \text{ \AA}^3$, Space Group; P-1 (#2), Z value; 2, D_{calc} ; 1.292 g/cm³, F_{000} ; 332.00, $\mu(\text{CuK}\alpha)$; 7.335 cm⁻¹, Intensity Measurement: Diffractometer; R-Axis RAPID, Radiation; CuK α ($\lambda = 1.54187 \text{ \AA}$), graphite monochromated, Voltage, Current; 40 kV, 100 mA, Temperature; 23.0 °C, Detector Aperture; 460.0 x 256.0 mm, Data Images; 45 exposures, ω oscillation Range ($\chi=54.0$, $\phi=0.0$); 80.0 - 260.0°, Exposure Rate; 360.0 sec./°, ω oscillation Range ($\chi=54.0$, $\phi=90.0$); 80.0 - 260.0°, Exposure Rate; 360.0 sec./°, ω oscillation Range ($\chi=54.0$, $\phi=180.0$); 80.0 - 260.0°, Exposure Rate; 360.0 sec./°, ω oscillation Range ($\chi=54.0$, $\phi=270.0$); 80.0 - 260.0°, Exposure Rate; 360.0 sec./°, Detector Position; 127.40 mm, Pixel Size; 0.100 mm, $2\theta_{\text{max}}$; 136.4°, No. of Reflections Measured; Total: 8887, Unique: 2867 ($R_{\text{int}} = 0.0714$), Corrections; Lorentz-polarization Absorption (trans. factors: 0.582 - 0.971), Secondary Extinction (coefficient: 9.71000e-003). Structure Solution; Direct Methods (SHELXT Version 2018/2), Refinement; Full-matrix least-squares on F^2 , Function Minimized; $\Sigma w (F_o^2 - F_c^2)^2$, Least Squares Weights; $w = 1 / [\sigma^2(F_o^2) + (0.1217 \cdot P)^2 + 0.0000 \cdot P]$ where $P = (\text{Max}(F_o^2, 0) + 2F_c^2) / 3$, $2\theta_{\text{max}}$ cutoff; 136.4°, Anomalous Dispersion; All non-hydrogen atoms, No. Observations (All reflections); 2867, No. Variables; 209, Reflection/Parameter Ratio; 13.72, Residuals: $R_1 (I > 2.00\sigma(I))$; 0.0728, Residuals: R (All reflections); 0.1272, Residuals: wR_2 (All reflections); 0.2300, Goodness of Fit Indicator; 0.930, Max Shift/Error in Final Cycle ; 0.000, Maximum peak in Final Diff. Map; 0.20 e⁻ / \AA^3 , Minimum peak in Final Diff. Map; -0.23 e⁻ / \AA^3 .

Deposition number CCDC-2047465 for **12**. Free copies of the data can be obtained via <http://www.ccdc.cam.ac.uk/conts/retrieving.html> (or from the Cambridge Crystallographic Data Center, 12 Union Road, Cambridge, CB2 1EZ, UK; Fax: +44 1223 336033; e-mail: deposit@ccdc.cam.ac.uk).

Selected Bond Lengths (Å)					
O1-C1	1.355(4)	O1-C9	1.458(3)	O2-C1	1.210(4)
O3-C18	1.193(4)	O4-C18	1.332(6)	O4-C19	1.440(4)
C1-C2	1.467(6)	C2-C3	1.336(4)	C2-C18	1.501(5)
C3-C4	1.479(4)	C4-C5	1.527(6)	C4-C9	1.538(6)
C4-C11	1.586(6)	C5-C6	1.519(6)	C6-C7	1.522(7)
C7-C8	1.516(8)	C8-C9	1.511(6)	C9-C10	1.539(6)
C10-C11	1.542(5)	C11-C12	1.500(6)	C12-C13	1.392(6)

C12-C17	1.382(5)	C13-C14	1.389(7)	C14-C15	1.362(5)
C15-C16	1.378(7)	C16-C17	1.381(7)		
Selected Bond Angles (°)					
C1-O1-C9	120.6(3)	C18-O4-C19	115.2(3)	O1-C1-O2	117.0(4)
O1-C1-C2	118.4(2)	O2-C1-C2	124.5(3)	C1-C2-C3	121.6(3)
C1-C2-C18	117.5(3)	C3-C2-C18	120.8(4)	C2-C3-C4	124.0(4)
C3-C4-C5	109.5(3)	C3-C4-C9	110.7(2)	C3-C4-C11	110.7(3)
C5-C4-C9	118.3(4)	C5-C4-C11	119.8(2)	C9-C4-C11	86.0(3)
C4-C5-C6	113.5(4)	C5-C6-C7	110.7(3)	C6-C7-C8	108.7(4)
C7-C8-C9	112.2(4)	O1-C9-C4	116.9(3)	O1-C9-C8	105.5(3)
O1-C9-C10	115.5(3)	C4-C9-C8	115.1(3)	C4-C9-C10	89.6(3)
C8-C9-C10	114.2(3)	C9-C10-C11	87.6(3)	C4-C11-C10	87.7(3)
C4-C11-C12	119.7(3)	C10-C11-C12	121.9(4)	C11-C12-C13	122.1(3)
C11-C12-C17	120.8(3)	C13-C12-C17	117.1(4)	C12-C13-C14	120.3(3)
C13-C14-C15	121.6(4)	C14-C15-C16	118.9(5)	C15-C16-C17	119.7(4)
C12-C17-C16	122.3(4)	O3-C18-O4	123.4(3)	O3-C18-C2	125.0(4)
O4-C18-C2	111.5(3)				

13: Colorless plates; mp 221.0-223.7 °C (diisopropyl ether); ¹H-NMR (300 MHz, CDCl₃) δ 3.87 (s, 2H), 3.79 (s, 6H), 2.32-2.09 (m, 6H), 2.00-1.85 (m, 2H), 1.81-1.50 (m, 8H).; ¹³C-NMR (125 MHz, CDCl₃) δ 169.0 (2C), 162.2 (2C), 148.5 (2C), 106.2 (2C), 53.5 (2C), 53.0 (2C), 45.8 (2C), 26.2 (2C), 25.8 (2C), 21.9 (2C), 21.8 (2C); IR (CHCl₃): 2945.1, 1755.1 cm⁻¹; LR-EIMS *m/z*: 416 (M⁺, 5.7), 209 (59), 208 (100), 180 (48), 177 (61), 176 (33), 121 (31).; HR-EIMS calcd for C₂₂H₂₄O₈: 416.1471. Found: 416.1475.

X-Ray Crystal Data: Crystal Color, Habit; colorless, prism, Crystal Dimensions; 0.300 x 0.200 x 0.150 mm, Crystal System; orthorhombic, Lattice Type; Primitive, Lattice Parameters; a = 17.9688(7) Å, b = 8.5912(3) Å, c = 13.4535(5) Å, V = 2076.88(13) Å³, Space Group; P2₁2₁2 (#18), Z value; 4, D_{calc}; 1.332 g/cm³, F₀₀₀; 880.00, μ(MoKα); 1.015 cm⁻¹, Intensity Measurement: Diffractometer; R-Axis RAPID, Radiation; MoKα (λ = 0.71075 Å), graphite monochromated, Voltage, Current; 50 kV, 100 mA, Temperature; -165.0 °C, Detector Aperture; 460.0 x 256.0 mm, Data Images; 44 exposures, ω oscillation Range (χ=45.0, φ=30.0); 130.0 - 190.0°, Exposure Rate; 90.0 sec./°, ω oscillation Range (χ=45.0, φ=180.0); 0.0 - 160.0°, Exposure Rate; 90.0 sec./°, Detector Position; 127.40 mm, Pixel Size; 0.100 mm, 2θ_{max}; 54.8°, No. of Reflections Measured; Total: 20098, Unique: 4722 (R_{int} = 0.0624), Corrections; Lorentz-polarization Absorption (trans. factors: 0.771 - 0.985), Secondary Extinction (coefficient:

6.99000e-003). Structure Solution; Direct Methods (SHELXT Version 2018/2), Refinement; Full-matrix least-squares on F^2 , Function Minimized; $\Sigma w (F_o^2 - F_c^2)^2$, Least Squares Weights; $w = 1 / [s^2(F_o^2) + (0.0294 \cdot P)^2 + 4.6023 \cdot P]$ where $P = (\text{Max}(F_o^2, 0) + 2F_c^2)/3$, $2\theta_{\text{max}}$ cutoff; 54.8° , Anomalous Dispersion; All non-hydrogen atoms, No. Observations (All reflections); 4722, No. Variables; 282, Reflection/Parameter Ratio; 16.74, Residuals: R1 ($I > 2.00\sigma(I)$); 0.0729, Residuals: R (All reflections); 0.1134, Residuals: wR2 (All reflections); 0.1850, Goodness of Fit Indicator; 1.129, Max Shift/Error in Final Cycle; 0.000, Maximum peak in Final Diff. Map; $0.37 \text{ e}^- / \text{\AA}^3$, Minimum peak in Final Diff. Map; $-0.31 \text{ e}^- / \text{\AA}^3$.

Deposition number CCDC-2047494 for **13**. Free copies of the data can be obtained via <http://www.ccdc.cam.ac.uk/conts/retrieving.html> (or from the Cambridge Crystallographic Data Center, 12 Union Road, Cambridge, CB2 1EZ, UK; Fax: +44 1223 336033; e-mail: deposit@ccdc.cam.ac.uk).

Selected Bond Lengths (Å)					
O1-C9	1.424(9)	O1-C1	1.344(8)	O2-C1	1.218(8)
O3-C10	1.219(8)	O4-C10	1.333(7)	O4-C11	1.454(10)
O5-C12	1.356(7)	O5-C20	1.423(7)	O6-C12	1.214(7)
O7-C21	1.219(7)	O8-C21	1.328(7)	O8-C22	1.448(8)
C9-C4	1.318(9)	C9-C8	1.477(10)	C10-C2	1.492(8)
C12-C13	1.496(8)	C13-C14	1.559(8)	C13-C14 ¹	1.578(8)
C13-C21	1.507(8)	C14-C15	1.484(8)	C15-C16	1.507(9)
C15-C20	1.324(9)	C16-C17	1.535(15)	C16-C17A	1.57(5)
C17-C18	1.45(2)	C18-C19	1.504(11)	C18-C17A	1.34(4)
C19-C20	1.480(10)	C1-C2	1.502(9)	C2-C3	1.557(8)
C2-C3 ²	1.570(8)	C3-C4	1.481(8)	C4-C5	1.497(9)
C5-C6	1.583(14)	C6-C7	1.453(14)	C7-C8	1.506(14)
Selected Bond Angles (°)					
C9-O1-C1	121.2(5)	C10-O4-C11	116.3(6)	C12-O5-C20	121.8(5)
C21-O8-C22	116.8(5)	O1-C9-C4	123.5(6)	O1-C9-C8	109.0(6)
C4-C9-C8	127.5(7)	O3-C10-O4	124.3(6)	O3-C10-C2	125.8(5)
O4-C10-C2	109.9(5)	O5-C12-O6	118.2(5)	O5-C12-C13	120.3(5)
O6-C12-C13	121.5(5)	C12-C13-C14	115.8(5)	C12-C13-C14 ¹	115.1(5)
C12-C13-C21	107.7(5)	C14-C13-C14 ¹	89.6(4)	C14-C13-C21	113.3(5)

C14 ¹ -C13-C21	114.8(5)	C13-C14-C13 ¹	89.2(4)	C13-C14-C15	115.3(5)
C13 ¹ -C14-C15	119.2(5)	C14-C15-C16	118.9(5)	C14-C15-C20	121.5(5)
C16-C15-C20	119.6(6)	C15-C16-C17	111.7(6)	C15-C16-C17A	110.1(12)
C16-C17-C18	112.1(9)	C17-C18-C19	116.5(9)	C19-C18-C17A	121.2(15)
C18-C19-C20	110.8(7)	O5-C20-C15	123.1(5)	O5-C20-C19	109.2(5)
C15-C20-C19	127.7(6)	O7-C21-O8	124.6(5)	O7-C21-C13	125.7(5)
O8-C21-C13	109.7(5)	O1-C1-O2	117.2(6)	O1-C1-C2	120.9(5)
O2-C1-C2	121.9(6)	C10-C2-C1	108.8(5)	C10-C2-C3	113.3(5)
C10-C2-C3 ²	116.5(5)	C1-C2-C3	114.8(5)	C1-C2-C3 ²	112.8(5)
C3-C2-C3 ²	89.7(4)	C2-C3-C2 ²	89.2(4)	C2-C3-C4	115.4(5)
C2 ² -C3-C4	120.2(5)	C9-C4-C3	121.0(6)	C9-C4-C5	119.8(6)
C3-C4-C5	119.3(5)	C4-C5-C6	110.9(6)	C5-C6-C7	111.8(8)
C6-C7-C8	109.5(8)	C9-C8-C7	110.8(7)	C16-C17A-C18	116(3)

COMPUTATIONAL METHODS: The candidate compounds with at most five hundred from the lowest energy or less than 40 kJ/mol difference from the lowest energy were generated with the molecular mechanics method at the MMFF level of theory in the Spartan'18 software, which automatically identifies conformational degrees of freedom (single bonds and flexible rings). The equilibrium geometries of the candidate compounds were sequentially recalculated with the semi-empirical method at the PM3 level of theory and the Hartree–Fock method at the 6-31G* level of theory. Finally, the lowest-energy structures were obtained with the DFT method at the ω B97X-D/6-31G* level of theory. The HOMO and LUMO levels of **6** and styrene were determined by DFT, and their molecular orbital coefficients were calculated by the Hartree–Fock method at the STO-3G level of theory with the optimized geometries of the lowest-energy structures calculated by DFT. The ¹H-NMR spectra of **11**, *epi-11*, **12**, *epi-12*, **14**, and **15** were calculated according to the Boltzmann weights of some of the candidate conformers calculated by DFT.

ACKNOWLEDGEMENTS

This research was supported in part by a Strategic Research Foundation Grant aided Project for Private Universities from the Ministry of Education, Culture, Sports, Science and Technology of Japan (MEXT) (S1511024L). We would like to thank Editage (www.edtage.com) for English language editing.

SUPPORTING INFORMATION

Supplementary data (analytical data, X-ray data, ORTEP drawing, and the copy of ¹H-NMR and ¹³C-NMR spectra) associated with this article can be found, in the online version, at URL: <https://www.heterocycles.jp/newlibrary/downloads/PDFsi/27109/102/2>.

REFERENCES AND NOTES

1. C. Ebner and E. M. Carreira, *Chem. Rev.*, 2017, **117**, 11651; Y.-Y. Fan, X.-H. Gao, and J.-M. Yue, *Sci. China Chem.*, 2016, **59**, 1126; P. Keglevich, A. Keglevich, L. Hazai, G. Kalas, and C. Szantay, *Curr. Org. Chem.*, 2014, **18**, 2037; D. Y.-K. Chen, R. H. Pouwer, and J.-A. Richard, *Chem. Soc. Rev.*, 2012, **41**, 4631; K. S. MacMillan and D. L. Boger, *J. Med. Chem.*, 2009, **52**, 5771; W. A. Donaldson, *Tetrahedron*, 2001, **57**, 8589.
2. S. Antonsen, R. B. Østby, and Y. Stenstrøm, 'Studies in Natural Products Chemistry,' Vol. **57**, ed. by Atta-ur-Rahman, Elsevier B. V., Amsterdam, 2018, pp. 1–40; J. Li, K. Gao, M. Bian, and H. Ding, *Org. Chem. Front.*, 2020, **7**, 136; J. C. J. M. D. S. Menezes and M. F. Diederich, *Eur. J. Med. Chem.*, 2019, **182**, 111637; T. V. Hansen and Y. Stenstrøm, 'Organic Synthesis: Theory Application,' Vol. **5**, Elsevier Science, ed. by T. Hudlicky, Oxford, 2001, pp. 1–38.
3. Y. Cohen, A. Cohen, and I. Marek, *Chem. Rev.*, 2020, DOI: 10.1021/acs.chemrev.0c00167; J. Xuan, X.-K. He, and W.-J. Xiao, *Chem. Soc. Rev.*, 2020, **49**, 2546; A. J. Craig and B. C. Hawkins, *Synthesis*, 2020, **52**, 27; D. K. Brownsey, E. Gorobets, and D. J. Derksen, *Org. Biomol. Chem.*, 2018, **16**, 3506; E. M. Budynina, K. L. Ivanov, I. D. Sorokin, and M. Y. Melnikov, *Synthesis*, 2017, **49**, 3035; M. A. Cavitt, L. H. Phun, and S. France, *Chem. Soc. Rev.*, 2014, **43**, 804; C. A. Carson and M. A. Kerr, *Chem. Soc. Rev.*, 2009, **38**, 3051; F. De Simone and J. Waser, *Chimia*, 2009, **63**, 162; F. De Simone and J. Waser, *Synthesis*, 2009, 3353.
4. I. Marek, A. Masarwa, P.-O. Delaye, and M. Leibelng, *Angew. Chem. Int. Ed.*, 2015, **54**, 414; J. Matsuo, *Tetrahedron Lett.*, 2014, **55**, 2589; N.-Y. Fu, S.-H. Chan, and H. N. C. Wong, 'Chemistry of Cyclobutanes,' Vol. I, ed. by Z. Rappoport and J. F. Liebman, John Wiley & Sons, Ltd., Chichester, 2005, pp. 357–440.
5. J. S. Ng and C. Liu, 'Encyclopedia of Reagents for Organic Synthesis,' 2nd ed., Vol. VI, ed. by L. A. Paquette, D. Crich, P. L. Fuchs, and G. A. Molander, John Wiley & Sons Ltd., Chichester, 2009, pp. 4336–4347; Y. G. Gololobov, A. N. Nesmeyanov, V. P. Lysenko, and I. E. Boldeskul, *Tetrahedron*, 1987, **43**, 2609; E. J. Corey and M. Chaykovsky, *J. Am. Chem. Soc.*, 1965, **87**, 1353; E. J. Corey and M. Chaykovsky, *J. Am. Chem. Soc.*, 1962, **84**, 867.
6. M. Yamashita, K. Okuyama, T. Kawajiri, A. Takada, Y. Inagaki, H. Nakano, M. Tomiyama, A. Ohnaka, I. Terayama, I. Kawasaki, and S. Ohta, *Tetrahedron*, 2002, **58**, 1497; M. Yamashita, K.

- Okuyama, I. Kawasaki, and S. Ohta, *Tetrahedron Lett.*, 1995, **36**, 5603.
7. M. Yamashita, T. Inaba, M. Nagahama, T. Shimizu, S. Kosaka, I. Kawasaki, and S. Ohta, *Org. Biomol. Chem.*, 2005, **3**, 2296; M. Yamashita, T. Inaba, T. Shimizu, I. Kawasaki, and S. Ohta, *Synlett*, 2004, 1897.
 8. T. D. Xuan and R. Teschke, *Molecules*, 2015, **20**, 16306; A. Goel and V. J. Ram, *Tetrahedron*, 2009, **65**, 7865; G. P. McGlacken and I. J. S Fairlamb, *Nat. Prod. Rep.*, 2005, **22**, 369.
 9. S. R. Turner, J. W. Strohbach, R. A. Tommasi, P. A. Aristoff, P. D. Johnson, H. I. Skulnick, L. A. Dolak, E. P. Seest, P. K. Tomich, M. J. Bohanon, M.-M. Horng, J. C. Lynn, K.-T. Chong, R. R. Hinshaw, K. D. Watenpaugh, M. N. Janakiraman, and S. Thaisrivongs, *J. Med. Chem.*, 1998, **41**, 3467.
 10. A. Garnica-Vergara, S. Barrera-Ortiz, E. Muñoz-Parra, J. Raya-González, A. Méndez-Bravo, L. Macías-Rodríguez, L. F. Ruiz-Herrera, and J. López-Bucio, *New Phytol.*, 2016, **209**, 1496.
 11. P. Mazzei, F. Vinale, S. L. Woo, A. Pascale, M. Lorito, and A. Piccolo, *J. Agric. Food Chem.*, 2016, **64**, 3538.
 12. V. Ahluwalia, S. Walia, O. P. Sati, J. Kumar, A. Kundu, J. Shankar, and Y. S. Paul, *Arch. Phytopathol. Plant Protect.*, 2014, **47**, 1063; A. Evidente, A. Cabras, L. Maddau, S. Serra, A. Andolfi, and A. Motta, *J. Agric. Food Chem.*, 2003, **51**, 6957.
 13. B. Wang, W. Huang, J. Zhou, X. Tang, Y. Chen, C. Peng, and B. Han, *Org. Biomol. Chem.*, 2017, **15**, 6548; J. S. Dickschat, *Nat. Prod. Rep.*, 2017, **34**, 310.
 14. R. Pratap and V. J. Ram, *Tetrahedron*, 2017, **73**, 2529; K. Kranjc and M. Kočevár, *ARKIVOC*, 2013, **i**, 333.
 15. T. Miura, S. Fujioka, H. Iwasaki, M. Ozeki, N. Kojima, and M. Yamashita, *Tetrahedron Lett.*, 2014, **55**, 1536; T. Miura, N. D. Yadav, H. Iwasaki, M. Ozeki, N. Kojima, and M. Yamashita, *Org. Lett.*, 2012, **14**, 6048.
 16. H. M. Zhang, K. Kawabata, H. Miyauchi, and T. Shimo, *Heterocycles*, 2012, **85**, 333; H. Miyauchi, C. Ikematsu, T. Shimazaki, S. Kato, T. Shinmyozu, T. Shimo, and K. Somekawa, *Tetrahedron*, 2008, **64**, 4108; W. Wang, T. Shimo, T. Shinmyozu, T. Iwanaga, and K. Somekawa, *Heterocycles*, 2006, **68**, 1381; T. Shimo, M. Kawamura, E. Fukushima, M. Yasutake, T. Shinmyozu, and K. Somekawa, *Heterocycles*, 2003, **60**, 23; T. Shimo, T. Uezono, T. Obata, M. Yasutake, T. Shinmyozu, and K. Somekawa, *Tetrahedron*, 2002, **58**, 6111; T. Obata, T. Shimo, S. Yoshimoto, K. Somekawa, and M. Kawaminami, *Chem. Lett.*, 1999, **28**, 181; T. Shimo, S. Ueda, and K. Somekawa, *J. Heterocycl. Chem.*, 1995, **32**, 341; T. Shimo, S. Matsuzaki, and K. Somekawa, *J. Heterocycl. Chem.*, 1994, **31**, 387; T. Shimo, S. Yamasaki, K. Date, H. Uemura, and K. Somekawa, *J. Heterocycl. Chem.*, 1993, **30**, 419; T. Shimo, K. Date, and K. Somekawa, *J. Heterocycl. Chem.*, 1992, **29**, 387; K. Somekawa,

- T. Shimo, and T. Suishu, *Bull. Chem. Soc. Jpn.*, 1992, **65**, 354; T. Shimo, J. Tajima, T. Suishu, and K. Somekawa, *J. Org. Chem.*, 1991, **56**, 7150; T. Shimo, T. Iwakiri, K. Somekawa, and T. Suishu, *J. Heterocycl. Chem.*, 1992, **29**, 199; T. Shimo, M. Yasuda, J. Tajima, and K. Somekawa, *J. Heterocycl. Chem.*, 1991, **28**, 745; T. Shimo, K. Somekawa, Y. Wakikawa, H. Uemura, O. Tsuge, K. Imada, and K. Tanabe, *Bull. Chem. Soc. Jpn.*, 1987, **60**, 621; K. Somekawa, T. Shimo, H. Yoshimura, and T. Suishu, *Bull. Chem. Soc. Jpn.*, 1990, **63**, 3456.
17. T. Shimo, H. Matsukubo, and H. M. Zhang, *Heterocycles*, 2012, **85**, 2531; S. T. McCracken, M. Kaiser, H. I. Boshoff, P. D. W. Boyd, and B. R. Copp, *Bioorg. Med. Chem.*, 2012, **20**, 1482; T. Shimo, S. Ueda, T. Suishu, and K. Somekawa, *J. Heterocycl. Chem.*, 1995, **32**, 727; I. Ortmann, S. Werner, C. Krueger, S. Mohr, and K. Schaffner, *J. Am. Chem. Soc.*, 1992, **114**, 5048; M. Van Meerbeck, S. Toppet, and F. C. De Schryver, *Tetrahedron Lett.*, 1972, **13**, 2247; R. D. Rieke and R. A. Copenhafer, *Tetrahedron Lett.*, 1971, **12**, 879.
18. D. Sarkar, N. Bera, and S. Ghosh, *Eur. J. Org. Chem.*, 2020, 1310; S. Poplata, A. Tröester, Y.-Q. Zou, and T. Bach, *Chem. Rev.*, 2016, **116**, 9748; A. G. Griesbeck and M. Franke, 'Comprehensive Organic Synthesis (2nd Ed.)', Vol. 5, ed. by P. Knochel and G. A. Molander, Pergamon Press, 2014, pp. 129-158; P. Margaretha, *Helv. Chim. Acta*, 2014, **97**, 1027; J. P. Hehn, C. Mueller, and T. Bach, 'Handbook of Synthetic Photochemistry,' ed. by A. Albini and M. Fagnoni, John Wiley & Sons Ltd., 2010, pp. 171-215; N. Hoffmann, 'Handbook of Synthetic Photochemistry,' ed. by A. Albini and M. Fagnoni, John Wiley & Sons Ltd., 2010, pp. 127-169.
19. M. Yamashita, N. D. Yadav, M. Nagahama, T. Inaba, Y. Nishino, K. Miura, S. Kosaka, J. Fukao, I. Kawasaki, and S. Ohta, *Heterocycles*, 2005, **65**, 2411.
20. DFT calculations were performed using Spartan'18 software (Wavefunction, Inc.).
21. I. Fleming, 'Frontier Orbitals and Organic Chemical Reactions (Frontier Kidoho Nyumon,' John Wiley & Sons, Ltd., 1976, K. Fukui Comp; Y. Takeuchi and S. Tomoda Tras. Kodansha Scientific Ltd., 1978, pp. 239-261.
22. Y.-H. Hsieh, H. Iwasaki, Y. Iwai, Y. Tanabe, R. Taketomo, S. Yamanishi, Y. Tanaka, N. Kojima, and M. Yamashita, *Chem. Pharm. Bull.*, accepted.